Ultra-dense WDM-PON 6.25 GHz spaced 8x1 Gb/s based on a simplified coherent-detection scheme

M. Presi,[1,*] **R. Corsini,**[1] **M. Artiglia,**[1] **and E. Ciaramella**[1]

[1]*Scuola Superiore Sant'Anna, TeCIP Institute, via G. Moruzzi, 1 - 56124 - Pisa - Italy*

[*]*marco.presi@sssup.it*

Abstract: We demonstrate experimentally a novel type of coherent low cost Gigabit-to-the-User Ultra-Dense-Wavelength Division Multiplexing (UD-WDM) PON, featuring 6.25 GHz channel spacing and long reach. Polarization-independent coherent detection is achieved by exploiting a novel scheme which requires only a 3×3 coupler, three photodiodes, basic analogue processing and a common DFB as local oscillator (LO). This avoids the conventional polarization diversity approach. The DFB LO is free running, i.e. not locked in frequency, and is tuned to detect any of the eight channels by simply changing its temperature in a range of 2° C. We achieve 70 km long-reach transmission plus 30 dB attenuation, for a total of $>$ 45 dB optical distribution network loss. This indicates that this solution could be effectively exploited to overlay existing PON infrastructures by UD-WDM.

OCIS codes: (060.2330) Fiber optics communications; (060.1660) Coherent communications.

References and links

1. S. Narikawa, H. Sanjoh, N. Sakurai, K. Kumozaki, and T. Imai, "Coherent wdm-pon using directly modulated local laser for simple heterodyne transceiver," ECOC 2005, paper Paper We3.3.2.
2. H. Rohde, S. Smolorz, E. Gottwald, and K. Kloppe, "Next generation optical access: 1 Gbit/s for everyone," ECOC 2009, Paper 10.5.5.
3. D. Lavery, R. Maher, D. S. Millar, B. C. Thomsen, P. Bayvel, and S. J. Savory, "Digital coherent receivers for long-reach optical access networks," J. Lightwave Technol. **31**, 609–620 (2013).
4. H. Rohde, S. Smolorz, S. Wey, and E. Gottwald, "Coherent optical access networks," OFC/NFOEC 2011, paper OTuB1.
5. H. Rohde, E. Gottwald, S. Rosner, E. Weis, P. Wagner, Y. Babenko, D. Fritzsche, and H. Chaouch, "Trials of a coherent UDWDM PON over field-deployed fiber: Real-time LTE backhauling, legacy and 100G coexistence," J. Lightwave Technol. **33**, 1644–1649 (2015).
6. J. Prat, M. Angelou, C. Kazmierski, R. Pous, M. Presi, A. Rafel, G. Vall-llosera, I. Tomkos, and E. Ciaramella, "Towards ultra-dense wavelength-to-the-user: the approach of the COCONUT project," in "Transparent Optical Networks (ICTON), 2013 15th International Conference on," (IEEE, 2013), paper Tu.C3.2.
7. L. G. Kazovsky, P. Meissner, and E. Patzak, "ASK multiport optical homodyne receivers," J. Lightwave Technol. **5**, 770–791 (1987).
8. M. Presi, F. Bottoni, R. Corsini, G. Cossu, and E. Ciaramella, "All DFB-based coherent udwdm pon with 6.25 GHz spacing and a $>$ 40 dB power budget," IEEE Photon. Technol. Lett. **26**, 107–110 (2013).
9. E. Ciaramella, "Polarization-independent receivers for low-cost coherent OOK systems," IEEE Photon. Technol. Lett. **26**, 548–551 (2014).
10. M. Presi, R. Corsini, and E. Ciaramella, "Experimental demonstration of a novel polarization-independent coherent receiver for PONs," OFC 2014 pp. W4G–3.
11. C. Xie, P. J. Winzer, G. Raybon, A. H. Gnauck, B. Zhu, T. Geisler, and B. Edvold, "Colorless coherent receiver using 3x3 coupler hybrids and single-ended detection," Opt. Express **20**, 1164–1171 (2012).

#237380 Received 8 May 2015; revised 4 Jul 2015; accepted 7 Jul 2015; published 20 Aug 2015

1. Introduction

Optical coherent transmission systems are expected to be soon introduced also in access networks, namely wavelength division multiplexing passive optical networks (WDM-PON) [1–4]. However, many of the proposed approaches are based on similar system solutions as for core networks, i.e. expensive optical and/or electronic devices (including high-resolution DAC based transmitters, ADCs and advanced digital signal processing [5]). In this work, we tackle this key issue and we focus on UDWDM-PON by means of coherent detection, realized by avoiding expensive narrow line-width lasers and digital signal processing [6]. We previously demonstrated that a 3×3 phase diversity receiver [7], realized with common DFBs and simple analog electrical processing, works effectively with Gigabit class intensity modulated signals in UDWDM-PON [8].

Furthermore, the receiver had very low sensitivity (-48 dBm) and required only a coarse control of the local oscillator, whose optical frequency could be detuned up to 1 GHz from the signal carrier frequency. Those two features made this scheme very attractive for deployment over splitter-based networks, where loss is high and devices with limited cost should be used [6]. However, this solution was still polarization-dependent. Recently a scheme for extending effectively this approach to a polarization-independent (PI) configuration was presented theoretically [9]: considering the previous phase-diversity receiver, with a symmetric 3×3 coupler, polarization-independent (PI) operation can be obtained if the incoming signal is split and injected into two arms of the coupler, , provided that the frequency detuning between the LO and the signal carrier is high enough (around 70% of the bitrate [10]). We preliminary assessed this receiver experimentally in single-channel operation [10], confirming that the PI implementation adds a negligible power penalty.

Here we extend this concept and prove it in more realistic conditions, that is in the 6.25 GHz UD-WDM grid. Given that the PI receiver is operated in intradyne regime the resilience to adjacent crosstalk is reduced as it will be explained later. Therefore its operation over a small grid is not trivial and should be demonstrated experimentally. To this aim, we realize a scheme that is compatible with the evolution scenario represented in Fig. 1 [6]. At the OLT, groups of 8 UD-WDM channels with 6.25 GHz spacing are multiplexed by cascading 8:1 couplers and a common AWG (with 50 GHz 3 dB bandwidth). At the ONU, a wavelength pre-selected laser allows selecting any of the eight UD-WDM channels in a given wavelength group. We note that this scheme allows co-existence with legacy networks (e.g. the G-PON) operating on different wavelength bands, without dedicated colored optical filters in the Optical Distribution Network (ODN) which is today composed only of power splitters.

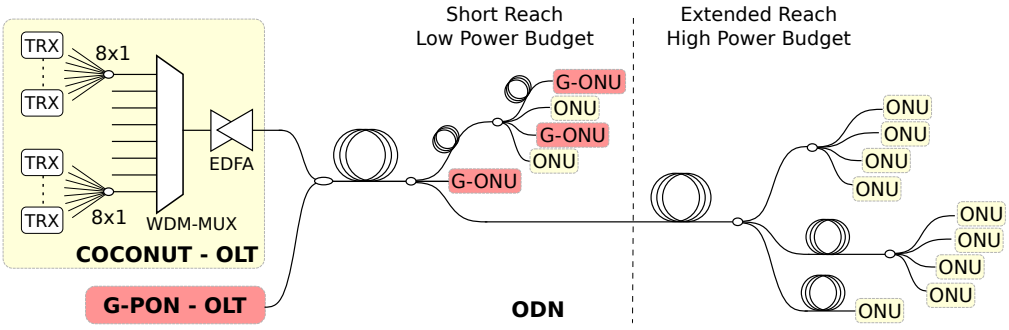

Fig. 1. Scheme and wavelength allocation plan of the considered UD-WDM network. TRX: Transceiver; EDFA Erbium Doped Fiber Amplifier; G-ONU: G-PON Optical Network Unit.

#237380 Received 8 May 2015; revised 4 Jul 2015; accepted 7 Jul 2015; published 20 Aug 2015

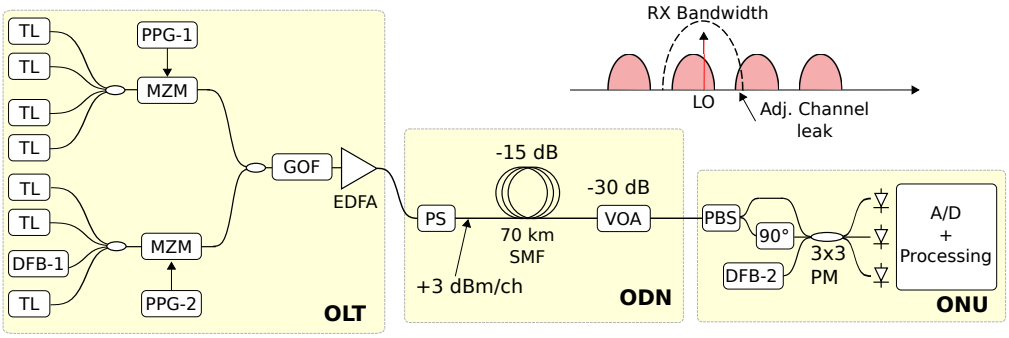

Fig. 2. Experimental setup. TL: Tunable Laser; DFB-1 and DFB-2: Distributed FeedBack lasers; MZM: Mach-Zehnder Modulator; PPG :Pulse Pattern Generator; GOF: Gaussian Optical Filter; EDFA: Erbium Doped Fiber Amplifier; PS: Polarization Scrambler; SMF: G-652 Single Mode Fiber; VOA: Variable Optical Attenuator; PBS: Polarization Beam Splitter; 3x3 PM: 3x3 Polarization Maintaining coupler; A/D: Analog-to-Digital Converter. Inset shows the relative position of the local oscillator and the selected WDM channel.

2. Experiments

The experimental setup that emulates the scenario described in Fig. 1, is illustrated in Fig. 2. At the OLT (optical line terminal), 8 CW lasers are coupled together by a network of optical couplers. The 8 λ are modulated in two groups of four (odd and even channels) by means of two Mach-Zehnder (MZ) intensity modulators. The MZs were driven by two independent PRBS sequences with different lengths (2^7-1 and $2^{15}-1$) so that adjacent channels carry uncorrelated data. The lasers (one DFB having 10 MHz linewidth and 7 tunable lasers acting as dummy channels) are set at the frequency spacing of 6.25 GHz around 1557 nm. In this experiment, no frequency control is implemented, so that the individual emission frequency wanders in a range of $\pm$100 MHz in respect to the nominal grid (i.e. the laser are operated in a set-and-forget mode). After the modulation stage odd and even channels are coupled together with orthogonal polarization states: in this way, the 8 channels are polarization interleaved, thus minimizing non-linear interactions among adjacent channels. This particular polarization arrangement might be useful only at the OLT side to increase the launch power of the down-stream channels. The upstream signals interact along the feeder fiber after a network of power splitting stages. Therefore they are coupled into the feeder power with an optical power which is well below the threshold for non-linear interactions: thus, no special control of the polarization of the upstream channels is required.

The UDWDM signals are then sent into a 50 GHz Gaussian filter emulating an usual WDM multiplexer with 100 GHz channel spacing and 50 GHz bandwidth. After that, an EDFA recovers the previous losses and then a variable optical attenuator (VOA) is used to vary the launch power per channel (thus resulting into values $\leq$ 3.5 dBm/channel). A polarization scrambler (0.5 dB insertion loss, changing randomly the SoP of the channels at a frequency of 6 kHz) is also added at the ODN input to test the behavior of the polarization independent receiver in a UDWDM environment. The signals are then launched into the ODN, made of a feeder fiber and optical attenuators, which emulate the losses due to the passive power splitter(s). The feeder fiber is made of two spools of G.652 single mode fibers, with a total length of 70 km and a total insertion loss of about 17 dB. At the ONU, the receiver is realized according to the second scheme presented in [9]. Here, in order to obtain stable operation, we realize the receiver choosing all the pigtailed components made all with polarization-maintaining fibers (PMFs): the incoming signal is first sent through a Polarization Beam Splitter (PBS), whose

#237380 Received 8 May 2015; revised 4 Jul 2015; accepted 7 Jul 2015; published 20 Aug 2015

PMF outputs are connected to 2 ports of a polarization maintaining 3×3 optical coupler. One of the PBS outputs is rotated by 90°, so that both the X and Y polarization components enter the slow axes of the 3×3 coupler (see Fig. 2). DFB-2, used as the local oscillator (LO) is connected to the 3 rd coupler port; it is also aligned to the coupler slow axis [9, 10]. The polarization rotation is implemented by proper alignment of the connectors at the PBS outputs: one of them has the key aligned to the slow axis, while the other has the key aligned to the fast axis). This arrangement of the PMFs used in the receiver avoids any dependency on the polarization control of the involved signals (in particular on the local oscillator). By doing this the receiver performance have been also improved significantly: the BER floor that was apparent in the results published in [10] has been removed thanks to this solution. The implementation based on polarization-maintaining components described above aims only at obtaining a stable system to demonstrating a proof-of-concept of the receiver in a WDM scenario. The present implementation is of course not cost-effective. In order to obtain cost-effective realizations for deployment scenarios, other platforms should be investigated such as integrated circuits or silica planar waveguides, as in the case of commercially available 90° hyrid couplers. The 3×3 coupler outputs are detected by three PIN+TIA diodes (2.5 GHz bandwidth), and a Real-Time Oscilloscope is used for A/D conversion (40 GS/s, 8 bit resolution) and processing [10]. As in [10], the processing consists in squaring and summing the differential output currents of the three photodiodes. By doing this, the direct-detection terms due to the WDM channels are miniimzed [11]. Once properly connected, the PMF components provide stable operation, thus in this configuration, the receiver is fully polarization independent and no manual polarization optimization/adjustment (e.g. usual polarization controller) is required inside the receiver. The receiver is used to detect each of the eight UD-WDM channels by tuning the LO. This is accomplished by varying the DFB operating temperature and bias current, for coarse and fine adjustment, respectively: in our case, the maximum temperature and current variations to select all 8 channels were of ± 2° C and ± 4 mA around the nominal values (20° C and 60 mA).

3. Receiver characterization

The LO was kept to an intradyne detuning of 900 MHz (± 100 MHz). The optimal detuning value has been predicted theoretically in [9]. In Fig. 3 we report the receiver tolerance to fluctuations of the signal-LO detuning as it is measured experimentally. The measurement is performed by keeping a fixed optical power to the receiver. For comparison, Fig. 3 also reports the tolerance in the case of single-polarization operation (white squares). The same measurement has been performed by using post-detection filters of different bandwidths. As can be seen, while the single polarization receiver is almost insensitive to detuning values up to 1 GHz [7] the

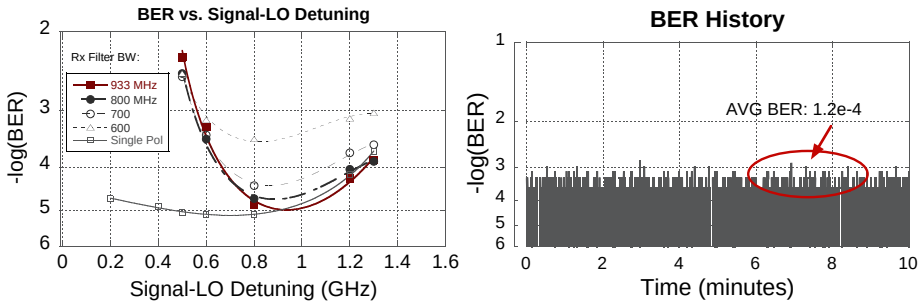

Fig. 3. Left: Tolerance of signal to local oscillator detuning in the proposed polarization receiver. for different bandwiths of the post-detection filter. Right: BER history log over 10 minutes of the polarization independent receiver.

#237380 Received 8 May 2015; revised 4 Jul 2015; accepted 7 Jul 2015; published 20 Aug 2015

polarization independent receiver works well in a reduced detuning range ($\pm$100 MHz around 900 MHz). When the signal-lo frequency detunings is small ($<$ 900 MHz), the interference term between the two splitted polarization components is fully in-band to the recovered signal. On the other hand, at high frequency detunings ($>$ 900 MHz) the interference terms falls outside the signal bandwidth and can be effectively filtered out by the post-detection filter. In symmary, the signal-LO detuning tolerance is bound on one side by the signaling rate and by the photodiode bandwidth on the other side. Such a tolerance could be in princinple extended by increasing the photodiodes bandwidth; however this would limit the minimum channel spacing in case of WDM operations as discussed briefly in the next section.

As explained in detail in [9], when the input signal is not polarization aligned with one of the PBS axis, a interference term appears at a frequency which is twice the signal-LO detuning value. This can be clearly seen in Fig. 4 where we report the detected signal as measured at point A in the receiver (see Fig. 2), i.e. before low-pass filtering: when the input polarization is aligned along one of the PBS axis, the envelope clearly shows an NRZ signal. On the other hand, when the input signal is linearly polarized at 45° with respect to the polarizer the reconstructed envelope contains a beating term at a twice the signal-lo detuning frequency [9]. The beating term is also clearly visible in the electrical spectrum of the trace, which is also reported in Fig. 4. Eye-diagrams of Fig. 4 show the action of the post-detection filter on the envelope recovered signal in the case of an input signal having a 45° polarization rotation. As can be seen a 933 MHz filter, which is usually employed in 1.25 Gb/s NRZ systems performs a very a good reshaping. Narrower post detection filters are not effective, as shown in Fig. 3.

The tolerance of 200 MHz on the signal-LO detuning allowed to avoid a fast frequency control on the local oscillator. In a real implementation of the receiver, such detuning might be implemented by means of a slow and very low bandwidth frequency locking-loop, acting on the local oscillator laser bias, this avoiding the need of a dedicated fast PLL circuit. In Fig. 3 we also report the BER fluctuations measured over the time when the receiver detects a signal of random varying polarization. Such a random polarization change is induced by a commercial polarization scrambler which provides for random polarization changes at a frequency of 6 kHz.

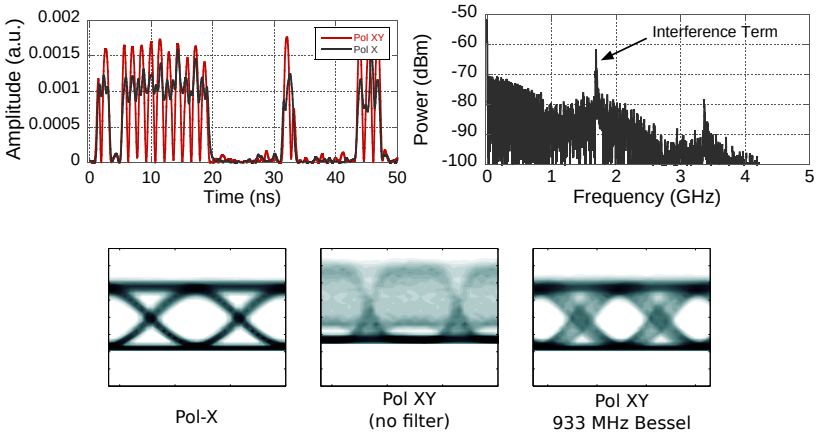

Fig. 4. Effect of the post-envelope low pass filter on the interfernce term generated when the received signal is not aligned to one of the PBS axis. Top left: detected envelopes when the signal is polarization aligned to the PBS axis ('PolX')or with a 45° angle ('PolXY'). Top right: spectrum of the received signal with 45° angle. These traces are recorded at point A in Fig. 2. Bottom eye diagram shows the received signal before and after low-pass filtering that suppresses the interference term.

#237380 Received 8 May 2015; revised 4 Jul 2015; accepted 7 Jul 2015; published 20 Aug 2015

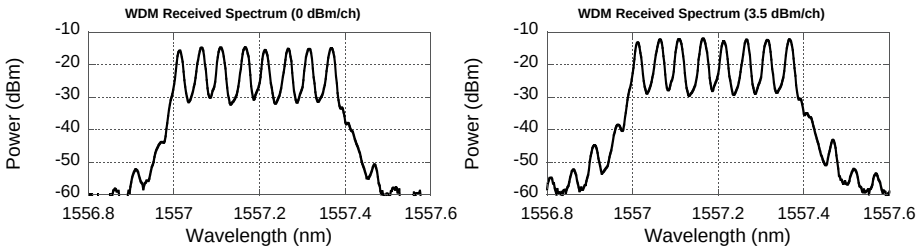

Fig. 5. Optical spectra at the end of the feeder fiber (RBW: 0.01 nm).

As can be seen, a stable average BER value is observed, i.e. there were no critical polarization states able to deteriorate the receiver performance.

4. WDM operations

There are two main sources of impairments when the proposed receiver is operated in a WDM environment: crosstalk from the adj. channels and the FWM effect occurring in the feeder segment of the network- As explained in the previous sections, the PI receiver works in a intradyne regime, a non-zero frequency offset between the signal and the local oscillator. As shown in the inset of Fig. 2 this might cause partial leaking of one of the adjacent channels. However, by selecting a proper bandwidth of the photodiodes in the receiver front-end, it is possible to avoid this effect and still operate on a 6.25 GHz grid without any penalty, as it will be shown in the following, where the performance of the receiver operated with a single or multiple input are reported. We therefore focused our attention on the non-linear interaction among the WDM channels.

The optical spectra of the UDWDM comb at the end of the feeder fiber are reported in Fig. 5, for different launch power/channel settings (0 and 3.5 dBm). As we can see, the Four-Wave-Mixing (FWM) is not significant at launch power up 0 dBm/ch. On the other side, even in the worst case of 3.5 dBm launch power/channel, the FWM products are about -25 dB below the channels. In order to verify the resilience to non-linear effects, we determined the performance of the middle grid channel ($\lambda = 1557.2$ nm, produced by DFB-1), as a function of the launch power. We report in Fig. 6 the bit error rate (BER) curves taken by varying the

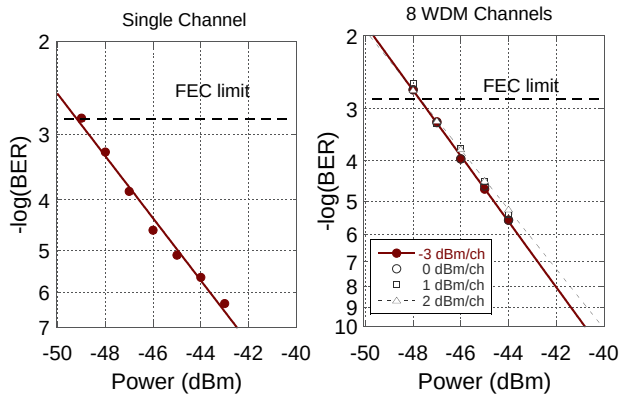

Fig. 6. Left: Receiver performance in the case of single-channel operation; Right: WDM performance at different launch power/channel at the OLT output.

#237380 Received 8 May 2015; revised 4 Jul 2015; accepted 7 Jul 2015; published 20 Aug 2015

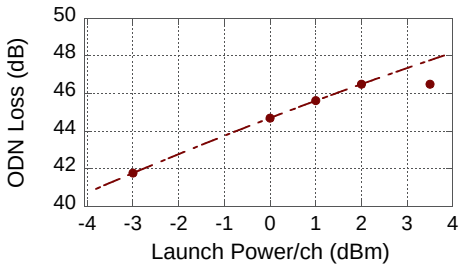

Fig. 7. Power budget vs launch power per channel at the ODN.

received power of the middle channel after the transmission line. In the same figure, we report, as reference, the performance of the receiver when only one channel is detected. As can be seen the power penalty measured for different launch power level is very low (< 0.5 dB at a BER of 10^{-6}). We note that when the receiver is operated with multiple signals at the input, a power penalty is introduced at the FEC level, which is probably due to a residual of the direct-detection terms (although we process the differential photocurrents in order to cancel-out the direct-detection terms such a cancellation is not perfect due to mismatch in photodiodes responsivities and frequency response). Nevertheless, with a sensitivity of -48 dBm at the FEC level (BER=$1.2x10^{-3}$), and a launch power of 2 dBm, this indicates a power budget of at least 50 dB over a 70 km reach. This result is in-line with what can be achieved by using state-of-the-art, higher-complexity, UDWDM-PON transceivers [5], although the proposed simplified approach pays in terms of spectral efficiency. Further increasing the launch power seems not to be beneficial in terms of power budget. This is reported in Fig. 7 where we report the measured ODN loss budget as a function of the launch power. As can be seen, when the launch power is increased to 3.5 dBm, the maximum value achievable with the EDFA used in the experiment, the system ODN loss does not increase. In this measurement, in order to obtain a conservative value, the sensitivity of the receiver was fixed at a BER of 10^{-5}.

We then characterize the performance of all the channels. We set the launch power to the maximum value (3.5 dBm/ch) and a fixed attenuation of 30 dB after the transmission line (47 dB total insertion loss). Also in these measurements the local oscillator power was fixed to 0 dBm, which resulted to be the optimal condition value for our receiver. Figure 8 reports the measured BER on individual channels, obtained by tuning the LO. As can be seen, all the channels show a BER between $1.5 \cdot 10^{-5}$ and $5 \cdot 10^{-6}$, which are well below the FEC threshold. By comparing this result with Fig. 6 we see the availability of at least 2 dB of margin to reach the

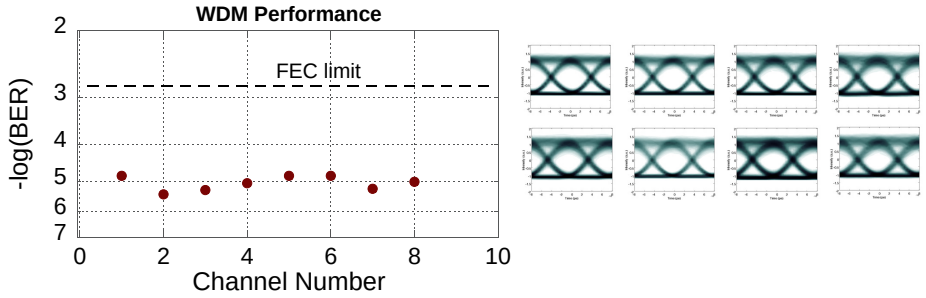

Fig. 8. BER values on each of the 8 channels after propagation along the ODN ($P_{launch} =$ 3.5 dBm/ch). Inset shows the eye diagrams recorded for each channel.

#237380 Received 8 May 2015; revised 4 Jul 2015; accepted 7 Jul 2015; published 20 Aug 2015

FEC level. The slight performance difference among the 8 channels is likely due by the non-uniformity of the individual channel power (set with a resolution of 0.5 dB). We also notice that the performance of the DFB-based channel cannot be distinguished from the TL ones, indicating that the use of a DFB as transmitter as well as LO does not introduce appreciable penalty. For completeness Fig. 8 also reports the eye- diagrams of all the 8 channels.

5. Conclusions

We presented a simplified polarization-independent coherent receiver suitable for access systems. The receiver avoids the use of polarization diversity but is still very robust against input polarization fluctuations. Thanks to an all-fiber implementation the receiver performance is improved with respect to that previously reported. Although requiring intradyne operation, the receiver can be used in ultra-dense WDM applications as the characterization in a 8*x*1.25 Gbit/s (gross-rate) UD-WDM systems with channel density as low as 6.25 GHz clearly shows. All the system is based on simple components such as common DFBs used as as a LO, which can select any of the incoming channels over a 6.25 GHz range (by a thermal tuning of 4°C). High power budget is demonstrated (50 dB), which is very promising for future deployment over today existing infrastructures, where high-loss splitters are present. This is particularly significant since only off-the-shelf components are required and all elements of the transmitter/receiver are in principle low-cost.

Acknowledgment

This work has been carried out under the framework of EU-funded FP7 project COCONUT (G.A. 318515)

#237380 Received 8 May 2015; revised 4 Jul 2015; accepted 7 Jul 2015; published 20 Aug 2015